Indian J. Phys. **77A** (4), 333–339 (2003)

AN INTERNATIONAL JOURNAL
IJPA

Photoemission study of Ba 2+ and Nd 3+ substitution for Ca 2+ in the BSCCO (2212) superconducting system

Kamlesh Kumari[1], R K Singhal[1], K B Garg[1]*, M Heinonen[2], J Leiro[2], Anurag Gupta[3] and S K Agarwal

[1]Condensed Matter Physics Laboratory, Department of Physics, University of Rajasthan, Jaipur 302 004, Rajasthan, India

[2]Applied Materials Science Laboratory, Department of Physics, University of Turku, 20014-Turku, Finland

[3]National Physical Laboratory, CSIR Complex, Pusa Road, New Delhi-110 012, India

E-mail krish35@sancharnet.in

Received 19 June 2002, accepted 8 April 2003

Abstract : The photoemission measurements have been carried out on the BSCCO (2212) superconducting system to understand the effect of substitution of trivalent impurity (Nd) for divalent Ca and the effect of substitution Ba that has a larger ionic radius than Ca. The two compounds have been characterized by XRD and resistivity measurements. The photoemission measurements have been made on the Bi 4*f*, Sr 3*d* and Ca 2*p* core levels. The core level spectra show some changes in their binding energies and fine structure - due to substitution in the two cases - which will be discussed in detail.

Keywords : Photoemission, cuprate superconductors, core levels, valence band, BSCCO

PACS Nos. : 79.60.Jv, 74.72.Hs

1. Introduction

The Bi-based cuprate superconductors are represented by the general formula $Bi_2Sr_2Ca_{n-1}Cu_nO_{(2n+4)+\gamma}$, the $n = 2$ being known as the 80 K (2212 phase). A lot of substitutional studies at different cationic sites have been made to understand the basic mechanisms that govern the superconducting properties [1–7]. If Cu is replaced by 3*d* elements in BSCCO, the substitution affects directly the CuO_2 planes. Extensive cationic substitutional studies are available for $La_{2-x}Sr_xCuO_4$ (LSCO), $YBa_2Cu_3O_{7-\delta}$ (YBCO) and Nd–Ce–Cu–O system [1–5]. A widely observed effect with respect to the incorporation of the 3*d* element is the suppression of T_c with increasing impurity concentration [6–8]. Our own study on Co-doped BSCCO, results in decrease of T_c with increasing Co concentration [9]. The doping of Y at Ca site, decreases the T_c as well as the Cu valence [10]. Also, it has been found that rare earth ions doping in Sr site of Bi-2201, is accompanied by incorporation of extra oxygens and enhancement of T_c upto 30 K [11]. By substituting rare earth elements for Ca in Bi-2212, a transition from superconductor to insulator is found to occur with progressive substitutions of rare earths and this transition has been attributed to a decrease in the carrier concentration [12–14]. Generally, there may be two reasons for superconductor to insulator transition. First, the substitution of trivalent impurity for divalent Ca kills holes and decreases the carrier concentration and second is the substitution of ion having different ionic radius than Ca, inducing pressure effects, thus changing the superconducting properties. It is very interesting to study these two effects separately taking the other as constant. Hence, we report herein a systematic study of the changes in the core level XPS spectra of $Bi_2Sr_2Ca_{1-x}Nd_xCuO_{8}$ ($x = 0.05, 0.2$) (where the ionic radius of Nd is same as Ca and the valence of Nd is +3 higher than the Ca) and $Bi_2Sr_2Ca_{1-x}Ba_xCuO_{8}$ ($x = 0.05, 0.2$) (where the valence of Ba is same and the ionic radius of Ba is higher than the ionic radius of Ca) samples in detail.

*Corresponding Author

2. Experimental

The samples of Nd and Ba doped BSCCO (2212) were prepared by solid state reaction method in a microprocessor controlled furnace (with temperature accuracy of ± 1°C at 1000°C). The starting materials were Bi_2O_3, $SrCO_3$, $CaCO_3$, Nd_2O_3, $BaCO_3$ and CuO powders with the purity of 4N (>99.99%). The powders were mixed well and calcined in air at 800°C for 12 hours. The mixing and calcination were repeated at 810°C and 815°C to ensure complete reaction. The reacted powder was then pressed into pellets and heated at 860°C for 48 hours followed by quenching to liquid nitrogen temperature.

The resistivity of the samples were measured by four-probe method in the temperature range 25–300 K.

The valence band and core level photoemission studies were carried out on an X-ray photoelectron spectrometer. The spectra were taken with non-monochromatic but monoenergetic AlK_α X-radiation (resolution was 0.9 eV and pass energy 35 eV). Energy scale and resolution calibration were made using sputter cleaned gold (Au 4*f* line at 84.0 eV). The vacuum was 5* 10^{-10} torr both in the preparation chamber and measuring chamber. Fresh surfaces needed for the measurements were obtained by mechanically scraping the sample surface in UHV. Scraped and cleaved surfaces show similar results, so the spectra have been taken on scraped surfaces. Scraping was done several times until there was no change in the amount of oxygen and carbon, which indicates surface contamination. No shift due to charging was observed in any of the core-levels recorded. The spectra were analyzed using a least square fitting photoemission program known as Rainbow-PC.

3. Results and discussion

From the resistivity measurements shown in Figure 1, the $T_{c,onset}$ is found to be nearly same for all the samples. Again, more or less ΔTc is same for pristine, low Nd-doped compound (Nd = 0.05) and high Ba-doped compound (Ba = 0.2), less for low Ba-doped compound (Ba = 0.05) and large for high Nd-doped compound (Nd = 0.2). The normal state resistivity also changes with doping. The compound with low-Nd doping (Nd = 0.05) shows an increase in normal state resistivity and the compound with high Nd-doping (Nd = 0.2) further show an increase in the normal state resistivity which is evident from the hole quenching by Nd 3+. The low Ba-doped compound (Ba = 0.05) shows a decrease in the normal state resistivity. The normal state resistivity of high Ba-doped compound (Ba = 0.2) increases as compared to low Ba-doped compound but is still lower than the pristine sample.

X-ray photoemission studies have been carried out on the core level electron states of Bi, Ca, Sr, Cu and oxygen and the valence band in the $Bi_2Sr_2Ca_{1-x}Nd_xCu_2O_{8}$ (x = 0.05, 0.2) and the $Bi_2Sr_2Ca_{1-x}Ba_xCu_2O_{8}$ (x = 0.05, 0.2) systems. The deconvoluted spectra of Bi 4*f*, Ca 2*p*, Sr 3*d*, Cu 2*p*, O 1*s*, Ba 3*d* and the valence band are given in the Figures (2–9) respectively.

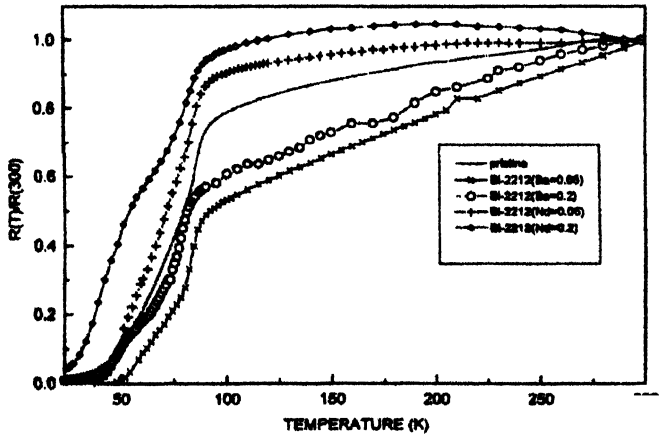

Figure 1. Resistivity measurements for pristine BSCCO (2212) and doped BSCCO (2212) for different Ba- and Nd-doping concentrations.

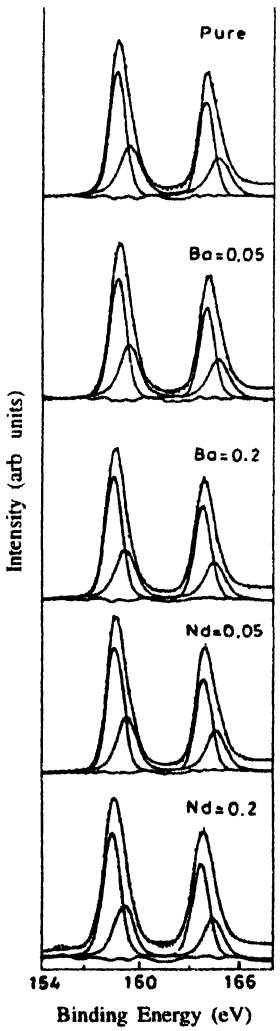

Figure 2. Bi 4*f* XPS spectra of BSCCO (2212) for different Ba- and Nd-doping concentrations.

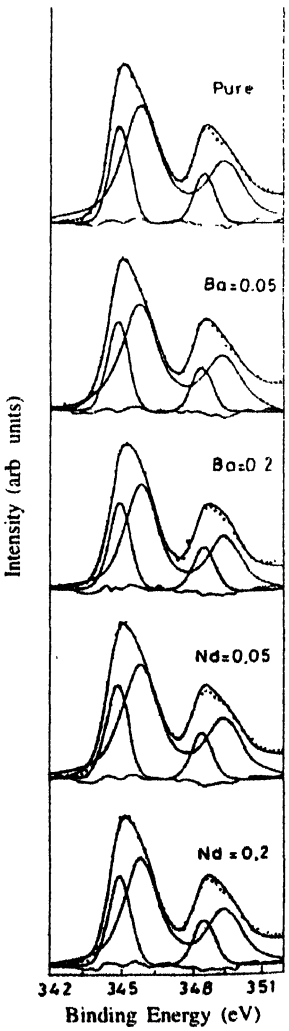

Figure 3. Ca 2*p* XPS spectra of BSCCO (2212) for different Ba- and Nd-doping concentrations

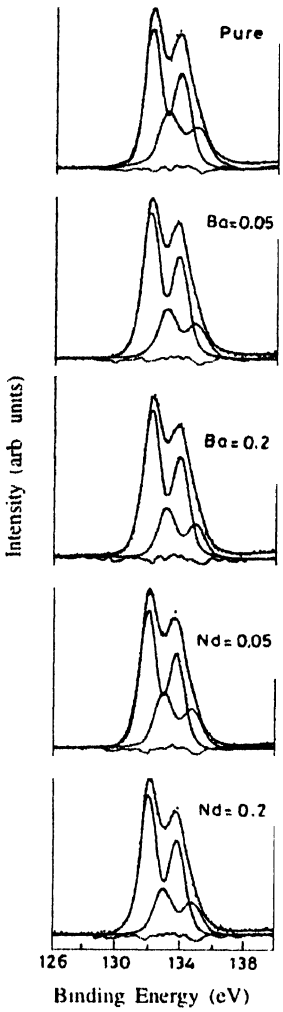

Figure 4. Sr 3*d* XPS spectra of BSCCO (2212) for different Ba- and Nd-doping concentrations

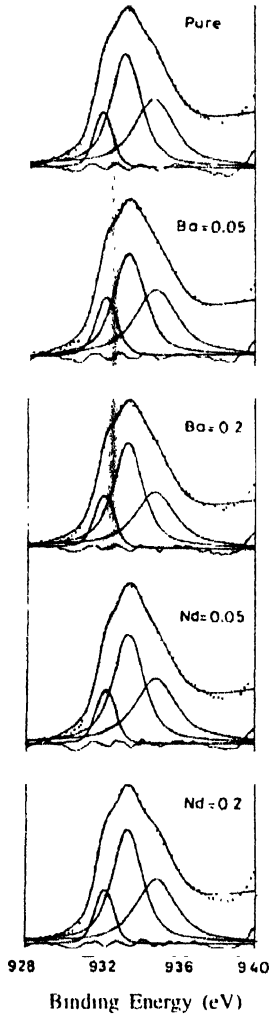

Figure 5. Cu 2*p* spectra of BSCCO (2212) for different Ba- and Nd-doping concentrations

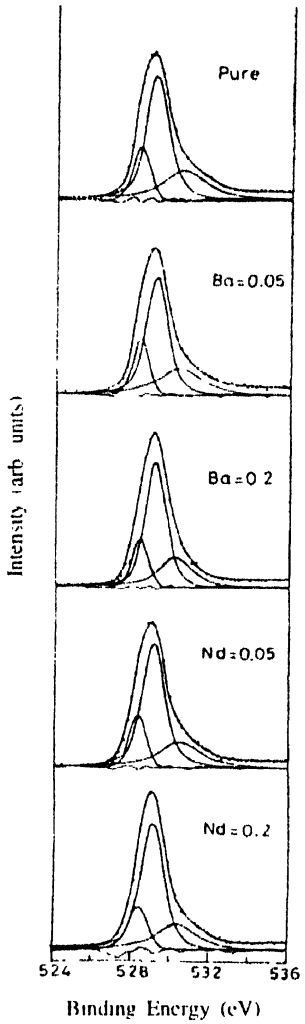

Figure 6. O 1s XPS spectra of BSCCO (2212) for different Ba- and Nd-doping concentrations

Bi 4f Core level :

Figure 2 shows the Bi 4*f* core level spectra for various doping concentrations of Ba and Nd. For pure Bi-2212, the Lower Binding Energy (LBE) peak is at 158.4 eV and Higher Binding Energy (HBE) peak is at 159.1 eV. The origin of the LBE is due to Bi in the Bi–O sheet and the HBE is due to Bi situated between the Bi–O and Cu–O sheets [15]. The LBE peak at 158.4 eV (for Bi_2O_3, the peak is at 158.5 eV) confirms Bi to be at oxidation state of 3+.

The HBE components are separated by 0.7 eV from the corresponding LBE components. In the case of pure BSCCO (2212) sample (x = 0), the intensity contribution from the LBE peak is 71% of the total intensity, which shows that Bi going to the Bi–O layers is 71% of the total Bi and Bi going between Bi–O and Cu–O layers is 29% of the total Bi. However, no appreciable shift in the binding energy of LBE and HBE is observed with progressive Ba and Nd doping concentrations. This shows that the average valence of Bi is 3+ and does not change with Ba and Nd doping. From Table 1, it is also clear that there is no systematic change in the ratio of the intensities of the components (I_{LBE}/I_{HBE}) with Ba and Nd doping. Hence, the chemical bond nature of Bi was not affected by Ca site doping. This only to be expected since Bi lies far away from the superconducting Cu-O_2 planes.

Ca 2p core level :

Figure 3 shows the Ca 2*p* spectra of the various doped samples. The spectra shows a doublet corresponding to transition from both Ca $2p_{3/2}$ and Ca $2p_{1/2}$ separated by 3.55 eV. The deconvoluted spectra of Ca $2p_{3/2}$ consist of two components LBE and HBE. In the case of pure BSCCO (2212) sample, the LBE is positioned at 344.82 eV and HBE is positioned at 345.75 eV. The LBE component has binding energy lower than metallic Ca and has assigned to the Ca atoms occupying the Sr site (between Bi–O layer and Cu–O layer) surrounded by four oxygen atoms. The binding energy of the HBE component is found to be the

Table 1. Binding energies of LBE and HBE for Bi $4f_{7/2}$, Ca $2p_{3/2}$ and Sr $3d_{5/2}$ and the ratios of their intensities.

Sample	Bi $4f_{7/2}$			Ca $2p_{3/2}$			Sr $3d_{5/2}$		
	LBE (eV)	HBE (eV)	$I_{LBE/HBE}$	LBE (eV)	HBE (eV)	$I_{LBE/HBE}$	LBE (eV)	HBE (eV)	$I_{LBE/HBE}$
Pure	158.36	159.09	2.44	344.82	345.75	0.84	131.935	132.913	2.48
Ba = 0.05	158.30	158.99	2.14	344.84	345.74	0.84	131.958	133.011	2.88
Ba 0.2	158.42	159.12	2.48	344.94	345.84	0.82	132.063	133.042	2.94
Nd 0.05	158.36	159.07	2.26	344.87	345.81	0.83	131.968	132.954	2.55
Nd 0.2	158.31	159.08	2.38	344.93	345.83	0.82	132.032	132.980	2.8

same as that in metallic Ca and is assigned to the Ca atoms at the Ca site (between two Cu–O planes) [15]. With both Ba and Nd doping, these components are found to shift to the high binding energies and thus indicate that Ca at both sites become more ionic in character. The positions of both the components and their relative intensity have been shown in the Table 1. We see that the ratio of the intensities of the components (I_{LBE}/I_{HBE}) decreases with Ba and Nd doping, but the decrease is very small. We see that for pure sample, 46% of the Ca is going at the Sr site and 54% of the Ca is going at the Ca site.

Sr 3d core level :

Figure 4 shows the Sr $3d$ spectra of the various doped samples which show a doublet corresponding to the transitions from Sr $3d_{5/2}$ and Sr $3d_{3/2}$ separated by 1.79 eV, the spin-orbit splitting. The deconvoluted spectra of Sr $3d_{5/2}$ show two doublets, LBE and HBE doublets. The binding energies of LBE and HBE of Sr $3d_{5/2}$ is 131.9 eV and 132.9 eV respectively. The binding energies of both the components are lower than that of $3d$ level in metallic Sr (134.3 eV). The four oxygen atoms around Sr are known to cause this decrease in the binding energies. The LBE and HBE components are assigned to Sr atoms at the Sr site (between the Bi–O layer and Cu–O layers) and at the Ca site (between the Cu–O layers) respectively [15]. For the undoped compound, the ratio of intensities of the components comes out as $I_{LBE}/I_{HBE} = 2.48$, which means that 71% of the Sr is going at the Sr site and 29% is going at the Ca site, as shown in Table 1. The interchangeability of Sr and Ca ions has been reported by many authors. With Ba and Nd doping, the relative site occupancy of Sr ion at the Sr site increases to 75% for Ba = 0.2 doping and 74% for Nd = 0.2. We can say on this account that Ba and Nd ion preferentially occupies Ca site, thus lowering the probability of Sr atom to occupy Ca site. We also observe a shift in the LBE and HBE to higher binding energies and the shift is 0.12 eV for Ba = 0.2 and 0.1 eV for Nd = 0.2. This shows that Sr atom becomes more ionic in character and goes to a valence state higher than 2+ with progressive Ba and Nd doping.

Cu 2p core level :

Figure 5 shows the Cu $2p$ spectra of Ba- and Nd-doped BSCCO (2212) samples. The spectra show well-screened spin-orbit split main lines $2p_{3/2}$ (~933 eV) and $2p_{1/2}$ (~953 eV) with their respective satellites at ~9 eV from each of them. The main peak, in general, represents the $2p3d^{10}\underline{L}$ and $2p3d^{10}\underline{L}^2$ final states while the satellite represents the $2p3d^9$ multiplet final states, where $2p$ denotes a core hole state and $\underline{L}$ signifies charge transfer from oxygen ligands to the Cu 2+ ions. The broad Cu $2p_{3/2}$ main line shows a shoulder at lower binding energy. The Cu $2p_{3/2}$ main line has been deconvoluted and shown in the figure. The main peak consists of three components, the central dominant peak at 933.2 eV is due to $2p3d^{10}\underline{L}$ final state and the higher binding energy peak at 934.7 eV is due to $2p3d^{10}\underline{L}^2$ final state which corresponds to Cu being in valence state higher than 2+. Many authors have attributed this to a trivalence state of Cu. The LBE peak at 932 eV shows the presence of Cu 1+ ($2p3d^{10}$) and this may originate from some other phase present in the sample. The binding energies of three peaks and their relative area have been shown in the Table 2.

Table 2. Binding energies of three deconvoluted peaks for Cu $2p_{3/2}$ and ratios of their area as a % of total area.

Sample	Cu $2p_{3/2}$		
	I peak (eV) ($2p3d^{10}$)	II peak (eV) ($2p3d^{10}\underline{L}$)	III peak (eV) ($2p3d^{10}\underline{L}^2$)
Pure	932.00	933.19	934.71
	11.64%	47.62%	40.73%
Ba = 0.05	932.11	933.33	934.74
	15.26%	43.72%	41.02%
Ba = 0.2	932.11	933.32	934.78
	13.8%	48.49%	37.71%
Nd = 0.05	932.06	933.25	934.69
	12.68%	46.97%	40.35%
Nd = 0.2	932.07	933.25	934.78
	12.36%	49.18%	38.46%

O 1s Core level :

Figure 6 shows the O 1*s* spectra of Ba- and Nd-doped BSCCO (2212) samples. The spectra consist of three peaks at binding energies at ~528.3 eV, ~529.1 eV and ~530.4 eV in all the samples. The lower binding energy peak at 528.3 eV has its origin from the oxygen atoms from the Sr–O or Cu–O layers [16] and is responsible for superconductivity. The energies and their weightage are given in the Table 3. The peak at energy 529.1 eV has its origin from Bi–O planes or it may be a impurity peak. The peak at energy 530.4 eV may arise due to the extra oxygen intercalated between the Bi–O layers [16] or may be due to surface degradation or grain boundary contamination [17].

Table 3. Binding energies of three deconvoluted peaks for O 1*s* and their relative weightage

Sample	O 1*s*		
	I peak	II peak	III peak
Pure	528.3	529.1	530.5
	15.4%	58.1%	26.5%
Ba = 0.05	528.3	529.1	530.4
	16.58%	53.97%	29.44%
Ba = 0.2	528.3	529.1	530.14
	15.3%	58.57%	26.07%
Nd = 0.05	528.3	529.1	530.5
	15.3%	59.8%	24.9%
Nd = 0.2	528.3	529.1	530.4
	15.3%	59.9%	24.8%

Ba 3d Core level :

Figure 7 shows the Ba 3*d* core level spectra of two Ba-doped compounds of BSCCO (2212). In both spectra, two peaks can be seen, the Lower Binding Energy (LBE) peak and the Higher Binding Energy (HBE) peak. For the low Ba-doped compound (Ba = 0.05), Lower Binding Energy (LBE) peak is at 778.3 eV and the Higher Binding Energy (HBE) peak is at 779.1 eV. Since Ca and Sr are interchangeable in their lattice sites and Ba has been doped for Ca, Ba can also go to both the lattice sites. Hence, the two peaks can be attributed to two lattice sites of Ba *i.e.*, LBE arises due to Ba at Sr site and HBE arises due to Ba at Ca site. From the table, we see that with increased Ba-doping, the binding energy of the peaks shifts to higher binding energy side and also, the intensity ratio of LBE to HBE (I_{LBE}/I_{HBE}) increases, which means that with increased Ba-doping Ba going at the Ca site decreases. For low Ba doping (Ba = 0.05) Ba going at the Ca site is 59% and for high Ba-doping Ba going at Ca site is 53%.

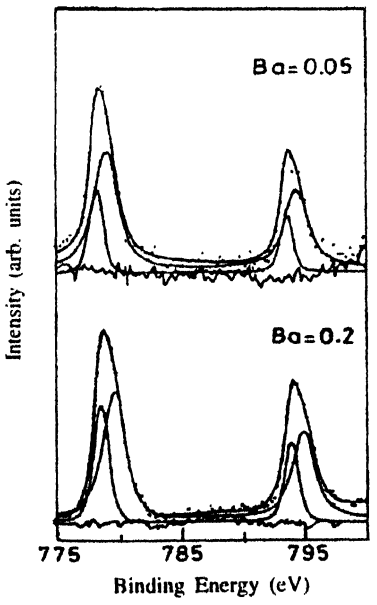

Figure 7. Ba 3*d* XPS spectra of BSCCO (2212) for two different Ba-doping concentrations.

Valence band

The XPS spectra of valence band of BSCCO in Figure 8 show a broad main band between 1.5 eV and 7.5 eV binding energy and a secondary peak centered at 11.5 eV. The spectrum is similar to what observed by Hillebrecht *et al* [18]. They have compared their spectrum with the carbon

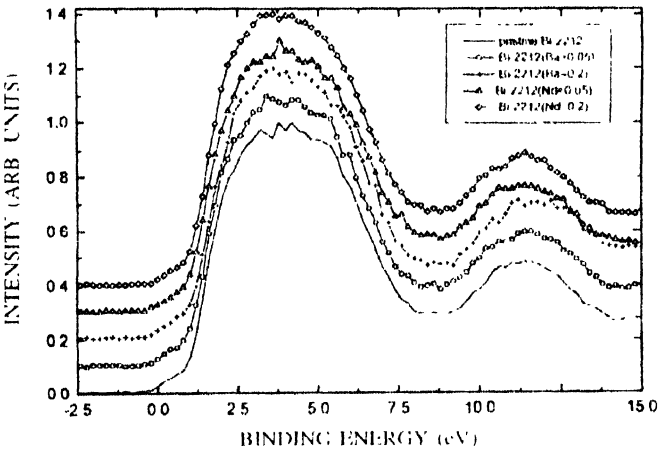

Figure 8. Valence band XPS spectra of BSCCO (2212) for different Ba-and Nd-doping concentrations

spectrum and concluded that all features correspond to the superconductor. By comparing our spectrum with their valence band spectrum, we can also conclude that all structures must be ascribed to the superconductor. The broad band between 1.5 eV and 7.5 eV comprises of Cu 3*d*, Bi 6*p*, Ca 3*d* and O 2*p* bands. A little contribution from Bi 6*s* is also present at the higher energy side of the main peak. The second peak at 11.4 eV has been observed in other superconductors also [19,20], and can be characterized by a two-hole satellite [18].

By comparing the spectra of all doped samples with the pure one, we can say that all spectra look alike. The only dissimilarity is at the higher energy side of the second peak for the sample (Ba = 0.2). This may be due to the

contribution coming from the Ba 5*p* bands and this contribution is negligible for the sample (Ba = 0.05) as Ba-content is very low in that sample.

The valence band spectra for all samples have been normalized and then deconvoluted (shown in Figure 9). Now, the area of the first peak will be a signature of density of holes near fermi level. It is clear that the area of the first peak decreases with Nd-doping, whereas in case of Ba-doping, we observe a little increase.

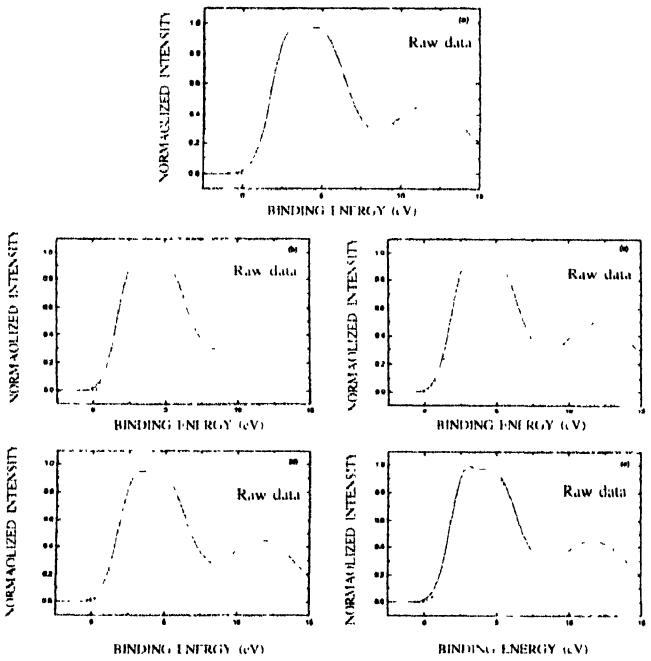

Figure 9. The valence band XPS spectra of BSCCO (2212) for different Ba- and Nd-doping concentrations have been normalized and then deconvoluted (a) pristine BSCCO (2212), (b) BSCCO (2212) (Ba = 0.05), (c) BSCCO (2212) (Ba = 0.2), (d) BSCCO (2212) (Nd = 0.05) and (e) BSCCO (2212) (Nd = 0.2)

Let us first confine attention to the Cu 2*p* results with reference to the pristine and low-doped compounds in Table 2. The observed decrease in the relative area of III peak (originating due to the presence of itinerant holes) with increasing Nd shows that the density of holes decreases with doping Nd. The decrease in the density of holes is due to the hole quenching by the Nd 3+. On the other hand, we observe an increase in the relative area of III peak with low Ba-doping, implying that there is an increase in the density of holes. However, there is a decrease in the relative area of III peak with both high Ba- and Nd-doping. These two compounds do not appear to be single phase and hence we do not discuss them any further. These results are quite consistent with the results obtained in the valence band spectra.

These results are also confirmed by the O 1*s* spectra where we observe three peaks out of which the first peak, which is at 528.3 eV is due to itinerant holes in the samples. Hence, the relative area of first peak is a measure of itinerant holes in the samples. From the Table 3, we observe that there is a decrease in the relative area of this peak for Nd-doped compounds and also for heavy Ba-doped compound. However for low Ba-doping it shows an increase, indicating a possible increase in number of itinerant holes in it. This may be responsible for the observed decrease in ΔTc.

4. Conclusions

The BSCCO (2212) superconductor with Ba- and Nd-doping has been synthesized and characterized by XRD and resistivity measurements. Bi-spectra show no shift in binding energy and confirms Bi to be in a valence state of 3+. Sr- and Ca-spectra confirm increase in binding energy and their fitting shows that Sr and Ca atoms become more ionic in character with progressive Ba- and Nd-doping. Also, the interchangeability of Ca and Sr ions results in the occupation of both sites by Ca site dopant. The Cu 2*p* and O 1*s* spectra show that low Ba-doping results in decrease in the transition width ΔTc as compared to all other studied samples. Nd-doping as expected, leads to deterioration in the superconducting behaviour of the samples.

References

[1] A V Narlikar, C V Narasimha Rao and S K Agarwal in *Studies of High Temperature Superconductors 1* (ed) A V Narlikar (New York : Nova Science) 341 (1989)

[2] G Hilscher, P Rogl, E Gratz, H Muller and P Fischer *Physica* **C158** (1988), G Hilscher, S Pollinger, L H Greene, G W Hull and W R McKinnon *Physica* **C167** 472 (1990)

[3] M Tarascon and B G Bagley in *Chemistry of Superconducting Materials* (ed) T Vanderah (Park Ridge, NJ Noyes) (1990)

[4] E Wang, J M Tarascon, L H Greene, G W Hull and W R McKinnon *Phys. Rev.* **B41** 6582 (1990)

[5] S Yamagata, K Adachi, M Onoda, H Fujishita, M Sera, Y Ando and M Sato *Solid State Commun.* **74** 177 (1990)

[6] K V R Rao, K B Garg, S K Agarwal, V P S Awana and A V Narlikar *Physica* **C192** 419 (1992)

[7] A Maeda, T Yabe, S Takebayashi, M Hase and K Uchinokura *Phys. Rev* **B41** 4112 (1990)

[8] N L Saini, B R Sekhar, P Srivastava, K B Garg, P Filip, K Mazenec, J Rusek and P Kuirek *J. Mat. Sci. Engg.* **B15** 9 (1992)

[9] N K Man, Kamlesh Kumari, S Venkatesh, T D Hien, N K Sinh, N X Phuc and K B Garg *Int. J. Mod. Phys.* **B13** 1655 (1999)

[10] B R Sekhar, N L Saini, P Srivastava and K B Garg *J. Phys. Chem. Solids* **55** 49 (1994)

[11] W A Groen *et al Solid State Commun.* **72** 697 (1989)

[12] H Yamanaka, H Enomoto, J S Shin, T Kishimoto, Y Takano, N Mori and H Ozaki *Jpn. J. App. Phys.* **30** 645 (1991); Y Shichi, Y Inoue, F Munakata and M Yamanaka *Phys. Rev.* **B42** 939 (1990)

[13] Mahmoud Khaled, P Srivastava, B R Sekhar, K B Garg, S K Agarwal, A V Narlıkar and F Studer *J. Phys Chem. Solids* **59** 777 (1998)

[14] B R Sekhar, P Srivastava, N L Saini, K V R Rao, S K Sharma and K B Garg *Physica* **C206** 139 (1993)

[15] S Kohiki, T Wada, S Kawashima, H Takagi, S Uchida and S Tanaka *Phys Rev.* **B38** 7051 (1988); S Kohiki, T Wada, S Kawashima, H Takagı, S Uchida and S Tanaka *Phys Rev* **B38** 8868 (1988)

[16] Bıju R Sekhar *PhD Thesis* (Department of Physics University of Rajasthan, Jaipur, Indıa) (1992)

[17] P Srivastava *et al Materi. Sci. Engg* **B22** 217 (1994)

[18] F U Hillebrecht, J Fraxedas, L Ley, H J Trdahl, J Zaanen, W Braun, M Mast, H Peterson, M Schaible, L C Bourne, P Pınsukanjana and A Zettl *Phys Rev.* **B39** 236 (1989)

[19] P D Johnson, S L Qui, F Garrett, B Sinkovic, N V Smith, R J Cava, C S Jec, D Nıcols, E Kaczanowicz, R E Salomon and J E Crow *Phys Rev* **B35** 8811 (1987), P Steiner, V Kinsinger, I Sander, B Siegwart, S Hufner and C Polıtis Z. *Phys* **B67** 19 (1987); M Onellıon, Y Chang, D W Nıles, R Joynt, G Margarıtondo, N G Stoffel and J M Tarascon *Phys. Rev* **B36** 819 (1987), J A Yarmoff, D R Clarke, W Drube, U O Karlsson, A Taleb-Ibrahımı and F J Himpsel *ibid* **B36** 3967 (1987)

[20] T Takahashı, F Maeda, H Arai, H Katayama-Yoshida, Y Okabe, T Suzukı, S Hosoya, A Fujımorı, T Shıdara, T Koıde, T Mıyahara, M Onoda, S Shamoto and M Sato *Phys Rev* **B36** 5686 (1987)